Products of the Gas-Phase Reaction of OH Radicals with Cyclohexane: Reactions of the Cyclohexoxy Radical

Sara M. Aschmann, Andrew A. Chew,† Janet Arey,*,† and Roger Atkinson*,†,‡

Statewide Air Pollution Research Center, University of California, Riverside, California 92521

Received: June 9, 1997; In Final Form: August 4, 1997⊗

Products of the gas-phase reactions of OH radicals with cyclohexane and cyclohexane-d_{12} in the presence of NO have been investigated using gas chromatography with flame ionization detection, combined gas chromatography−mass spectrometry, and in situ direct air-sampling atmospheric pressure ionization tandem mass spectrometry (API-MS). Cyclohexanone and cyclohexyl nitrate (and their deuterated analogues) were identified and quantified, with formation yields of cyclohexanone and cyclohexyl nitrate from the cyclohexane reaction of 0.321 ± 0.035 and 0.165 ± 0.021, respectively, and with cyclohexanone-d_{10} and cyclohexyl nitrate-d_{11} formation yields from the cyclohexane-d_{12} reaction of 0.156 ± 0.017 and 0.210 ± 0.025, respectively. The remaining products must arise from the decomposition and/or isomerization reactions of the intermediate cyclohexoxy radical. API-MS analyses of the cyclohexane and cyclohexane-d_{12} reactions showed the formation of cyclohexanone and cyclohexyl nitrate (and their deuterated analogues), together with ion peaks attributed to $HC(O)CH_2CH_2CH_2CH_2CH_2ONO_2$ (formed from NO addition to the $HC(O)CH_2CH_2CH_2CH_2CH_2OO^\bullet$ radical formed after decomposition of the cyclohexoxy radical) and $HC(O)CH_2CH(OH)CH_2CH_2CHO$ (formed after isomerization of the $HC(O)CH_2CH_2CH_2CH_2CH_2O^\bullet$ radical). No evidence for isomerization of the cyclohexoxy radical was obtained from the API-MS analyses. The reactions of the cyclohexoxy radical are discussed and the data extended to the reactions of the cyclopentoxy and cycloheptoxy radicals formed from cyclopentane and cycloheptane.

Introduction

Alkanes, including cycloalkanes, are important constituents of gasoline fuels, vehicle exhaust emissions, and ambient air in urban areas.[1−6] In the troposphere, alkanes and cycloalkanes react with the hydroxyl (OH) radical,[7−9] with the formation of alkoxy ($RO^\bullet$) radicals as intermediates in the degradation reaction sequences.[9] For example, in the presence of NO the reactions leading to the formation of alkoxy radicals are[9]

$$OH + RH \rightarrow H_2O + R^\bullet \tag{1}$$

$$R^\bullet + O_2 \xrightarrow{M} RO_2^\bullet \tag{2}$$

$$RO_2^\bullet + NO \xrightarrow{M} RONO_2 \tag{3a}$$

$$RO_2^\bullet + NO \rightarrow RO^\bullet + NO_2 \tag{3b}$$

Subsequent reactions of the alkoxy radicals determine the products formed from the tropospheric degradations of alkanes and cycloalkanes,[9,10] and these involve reaction with O_2, unimolecular decomposition, and isomerization,[9,10] as shown in Schemes 1−3, respectively, for the cyclohexoxy radical formed from cyclohexane. Although there is now a quantitative or semiquantitative understanding of the reactions of acyclic alkoxy radicals formed from alkanes,[10] there are only few data available concerning the tropospheric reactions of alkoxy radicals formed from the cycloalkanes.[11−15]

The reaction of the OH radical with cyclohexane in the presence of NO leads to the formation of cyclohexanone and cyclohexyl nitrate, with reported formation yields of ∼0.23−0.35[11,15] and 0.09−0.16,[11,16] respectively. The remaining products have not been identified or quantified but must arise from the decomposition and/or isomerization reactions of the

SCHEME 1

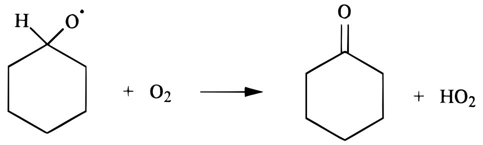

SCHEME 2

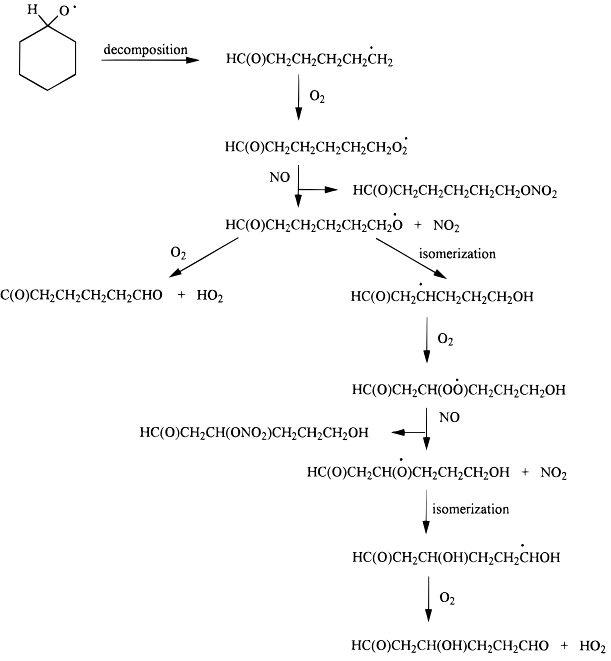

---

† Also Environmental Toxicology Graduate Program.

‡ Also Department of Chemistry, University of California, Riverside, CA 92521.

* To whom correspondence should be addressed.

⊗ Abstract published in *Advance ACS Abstracts,* September 15, 1997.

S1089-5639(97)01869-0 CCC: $14.00

SCHEME 3

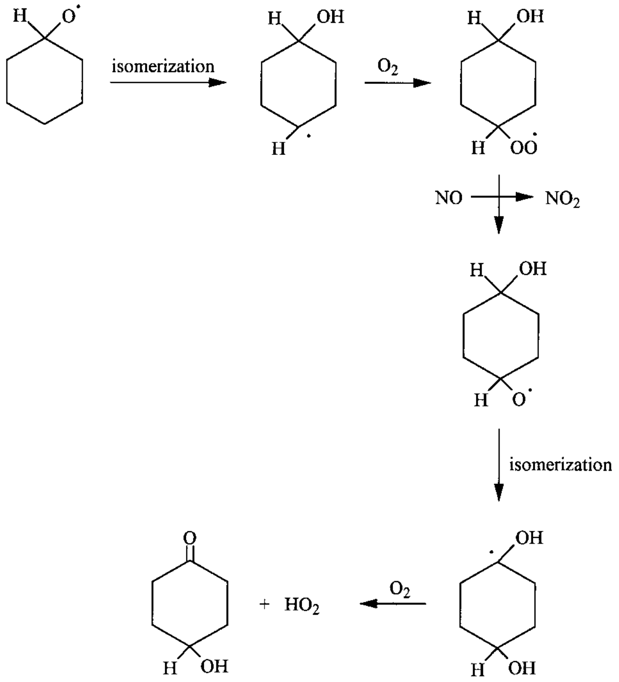

intermediate cyclohexoxy ($C_6H_{11}O^•$) radical. The expected reactions after the decomposition and isomerization of the cyclohexoxy radical are shown in Schemes 2 and 3, respectively, with certain reaction pathways being omitted (for example, decomposition of the $HC(O)CH_2CH_2CH_2CH_2CH_2O^•$ radical in Scheme 2) based on estimation of the relative importance of the reactions of certain alkoxy radicals.[10]

In this work we have used gas chromatography with flame ionization detection (GC-FID), combined gas chromatography−mass spectrometry (GC−MS), and in situ direct air sampling atmospheric pressure ionization tandem mass spectrometry (API-MS) to investigate the atmospheric chemistry of the OH radical-initiated reactions of cyclohexane and cyclohexane-d_{12} in the presence of NO.

Experimental Section

All experiments were carried out in 7000−7900 L Teflon chambers, each equipped with two parallel banks of black-lamps for irradiation and with a Teflon-coated fan to ensure rapid mixing of reactants during their introduction into the chamber. Products of the reactions of the OH radical with cyclohexane and cyclohexane-d_{12} in the presence of NO, at 298 ± 2 K and 740 Torr total pressure of purified air at ~5% relative humidity, were analyzed by GC-FID and by API-MS. Separate sets of experiments were carried out for each of these analytical methods.

Hydroxyl radicals were generated by the photolysis of methyl nitrite (CH_3ONO) in air at wavelengths greater than 300 nm,[17] and NO was added to the reactant mixtures to suppress the formation of O_3 and of NO_3 radicals.[17] The initial CH_3ONO, NO, and cyclohexane (or cyclohexane-d_{12}) concentrations were 2.4×10^{14}, 2.4×10^{14}, and $(2.27-2.45) \times 10^{13}$ molecule cm^{-3}, respectively, for the experiments with GC-FID analyses, and 4.8×10^{13} molecule cm^{-3} of each reactant for the experiments with API-MS analyses. Irradiations were carried out at 20% of the maximum light intensity (corresponding to an NO_2 photolysis rate of $\sim 2.5 \times 10^{-3}$ s^{-1}) for 15−45 min for the experiments with analyses by GC-FID and at the maximum light intensity for 2−3 min (cyclohexane) and 5−7.5 min (cyclohexane-d_{12}) for the experiments with in situ API-MS analyses.

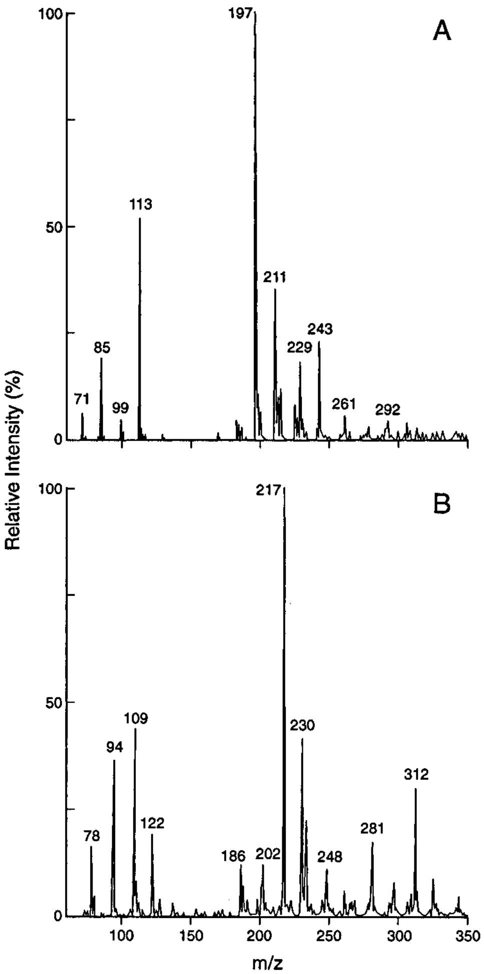

Figure 1. API-MS spectra of irradiated CH_3ONO−NO−cyclohexane−air (A) and CH_3ONO−NO−cyclohexane-d_{12}−air (B) mixtures.

The concentrations of cyclohexane and the products cyclohexanone and cyclohexyl nitrate were measured by GC-FID. For the analysis of cyclohexanone and cyclohexyl nitrate, 100 cm^3 volume gas samples were collected from the chamber onto Tenax-TA solid adsorbent with subsequent thermal desorption at ~225 °C onto a 30 m DB-1701 megabore column held at 0 °C and then temperature programmed to 200 °C at 8 °C min^{-1}. For the analysis of cyclohexane, gas samples were collected from the chamber in a 100 cm^3 all-glass, gastight syringe and introduced via a 1 cm^3 volume stainless steel loop and gas-sampling valve onto a 30 m DB-5 megabore column held at −25 °C and then temperature programmed at 8 °C min^{-1}. Calibrations of the GC-FID response factors for cyclohexane, cyclohexanone, and cyclohexyl nitrate were carried out as described previously for similar compounds.[18,19] Gas samples were also collected from the chamber onto Tenax solid adsorbent for subsequent thermal desorption and analysis by GC-MS, using a 30 m DB-1701 fused silica column in a Hewlett-Packard (HP) 5890 GC interfaced to an HP 5971 mass selective detector operating in the scanning mode.

For the API-MS analyses, a 7000 L Teflon chamber was interfaced to a PE SCIEX API III MS/MS direct air-sampling atmospheric pressure ionization tandem mass spectrometer (API-MS). The chamber contents were sampled through a 25 mm diameter × 75 cm length Pyrex tube at ~20 L min^{-1} directly into the API mass spectrometer source. The operation of the API-MS in the MS (scanning) and MS/MS [with collision-activated dissociation (CAD)] modes has been described elsewhere.[20−22] Use of the MS/MS mode with CAD allows the "daughter ion" or "parent ion" spectrum of a given ion peak

TABLE 1: Potential Products Formed from the OH Radical-Initiated Reaction of Cyclohexane and Cyclohexane-d_{12} in the Presence of NO (see Schemes 1−3) and Experimental Observations from in Situ API-MS and API-MS/MS Analyses

products[a]	API-MS data	other evidence
	Reaction 3a	
cyclohexyl nitrate M_1 (MW 145)	$[M_1 + H] = 146$ (v weak)	GC-FID quantification. MS/MS of 146 u ion peak (Figure 2) shows loss of NO_2 and NO_2^+ fragment.
cyclohexyl nitrate-d_{11} (MW 156)	$[M_1 + H] = 157$ (v weak)	GC-FID quantification. MS/MS of 157 u ion peak shows loss of NO_2 and NO_2^+ fragment.
	Reaction Scheme 1	
cyclohexanone M_2 (MW 98)	$[M_2 + H] = 99$ $[M_2 + M_2 + H] = 197$ $[M_2 + M_5 + H] = 229$ $[M_2 + M_5 + H - H_2O] = 211^b$	GC-FID quantification. MS/MS of 197, 211, and 229 u ion peaks, with parent of 99 observed at 197 and 211 u.
cyclohexanone-d_{10} (MW 108)	$[M_2 + H] = 109$ $[M_2 + M_2 + H] = 217$ $[M_2 + M_5 + H] = 248$ $[M_2 + M_5 + H - HDO] = 230$	GC-FID quantification. MS/MS of 230 and 248 u ion peaks.
	Reaction Scheme 2	
$HC(O)CH_2CH_2CH_2CH_2CH_2ONO_2$ M_3 (MW 161)	$[M_3 + H] = 162$ (v weak) $[M_3 + M_5 + H] = 292$	MS/MS of 162 u ion peak shows loss of NO_2 and NO_2^+ fragment. MS/MS of 292 u ion peak shows loss of NO_2.
$DC(O)CD_2CD_2CD_2CD_2CD_2ONO_2$ (MW 172)	$[M_3 + H] = 173$ (weak) $[M_3 + M_5 + H] = 312$ $[M_3 + M_2 + H] = 281$	MS/MS of 312 u ion peak shows loss of NO_2. MS/MS of 281 u ion peak.
$HC(O)CH_2CH_2CH_2CH_2CHO$ M_4 (MW 114)	$[M_4 + H] = 115$ (v weak) $[M_4 + M_2 + H] = 213$	MS/MS of 115 u ion peak (see Figure 4). Parent of 115 u was 213 u $[M_4 + M_2 + H] = 213$. MS/MS of 213 u ion peak.
$DC(O)CD_2CD_2CD_2CD_2CDO$ (MW 124)	$[M_4 + H] = 125$ $[M_4 + M_2 + H] = 233$	MS/MS of 125 u ion peak (see Figure 4) with HDO loss (and not H_2O loss). Parent of 125 u was 233 u. MS/MS of 233 u ion peak.
$HC(O)CH_2CH(ONO_2)CH_2CH_2CH_2OH$ (MW 177)		No evidence for formation.
$DC(O)CD_2CD(ONO_2)CD_2CD_2CD_2OH^d$ (MW 187)		No evidence for formation.
$HC(O)CH_2CH(OH)CH_2CH_2CHO$ M_5 (MW 130)	$[M_5 + H] = 131$ (v weak) $[M_5 + H - H_2O] = 113^b$ $[M_5 + M_5 + H] = 261$ $[M_5 + M_5 + H - H_2O] = 243^b$ $[M_5 + M_2 + H] = 229$ $[M_5 + M_2 + H - H_2O] = 211^b$	MS/MS of 131 u ion peak (see Figure 3). MS/MS of 211 and 229 u ion peaks. MS/MS of 243 and 261 u ion peaks.
$DC(O)CD_2CD(OH)CD_2CD_2CDO$ (MW 139)	$[M_5 + H] = 140^c$ (v weak) $[M_5 + H - H_2O] = 122^{b,c}$ $[M_5 + M_2 + H] = 248$ $[M_5 + M_2 + H - H_2O] = 230^c$	MS/MS of 140 u ion peak (see Figure 3). MS/MS of 230 and 248 u ion peaks.
	Reaction Scheme 3	
4-hydroxycyclohexanone (MW 114)	expect strong 97 u peak (not seen)	No evidence for formation (see text).
4-hydroxycyclohexanone-$d_9{}^d$ (MW 123)		No evidence for formation (see text).

[a] M_i has been used to refer to the products of both the cyclohexane and cyclohexane-d_{12} reactions. [b] Strong $[M + H - H_2O]^+$ fragment ion peaks are expected for hydroxy-containing compounds. [c] Expect loss of mainly H_2O and not HDO or D_2O. [d] After expected rapid −OD to −OH exchange.

observed in the MS scanning mode to be obtained.[20−22] The positive ion mode was used for all API-MS and API-MS/MS analyses, with protonated water hydrates ($H_3O^+(H_2O)_n$) ($n \approx 3-6$ at 298 K and ∼5% relative humidity[23]) generated by the corona discharge in the chamber diluent gas being responsible for the protonation of analytes,

$$H_3O^+(H_2O)_n + M \rightarrow MH^+(H_2O)_m + (n - m + 1)H_2O \qquad (4)$$

where M is the neutral analyte of interest. Ions are drawn by an electric potential from the ion source through the sampling orifice into the mass-analyzing first quadrupole or third quadrupole. For these experiments, the API-MS instrument was operated under conditions that favored the formation of dimer ions in the ion source region.[24] Neutral molecules and particles are prevented from entering the orifice by a flow of high-purity nitrogen ("curtain" gas), and as a result of the declustering action of the curtain gas on the hydrated ions, the ions that were mass-analyzed were mainly protonated molecular ions ($[M + H]^+$) and their protonated homo- and heterodimers.[20−22,24]

The chemicals used, and their stated purities, were the following: cyclohexane (high-purity solvent grade), American Burdick and Jackson; cyclohexane-d_{12} (99.5% atom D) and cyclohexanone (99.8%), Aldrich Chemical Co.; cyclohexyl nitrate, Fluorochem, Inc.; NO (≥99.0%), Matheson Gas Products. Methyl nitrite was prepared and stored as described previously.[17]

Results and Discussion

API-MS/MS Analyses. A series of $CH_3ONO-NO-$cyclohexane−air and $CH_3ONO-NO-$cyclohexane-d_{12}−air irradiations were carried out with API-MS analyses. The API-MS spectra of the irradiated mixtures are shown in parts A and B of Figure 1 for the cyclohexane and cyclohexane-d_{12} reactions, respectively. Based on Schemes 1−3 and the formation of cyclohexyl nitrate from the reaction of the cyclohexyl peroxy radical with NO (reaction 3a), seven potential products, their molecular weights, and the corresponding deuterated species expected from the reaction of cyclohexane-d_{12} are listed in Table

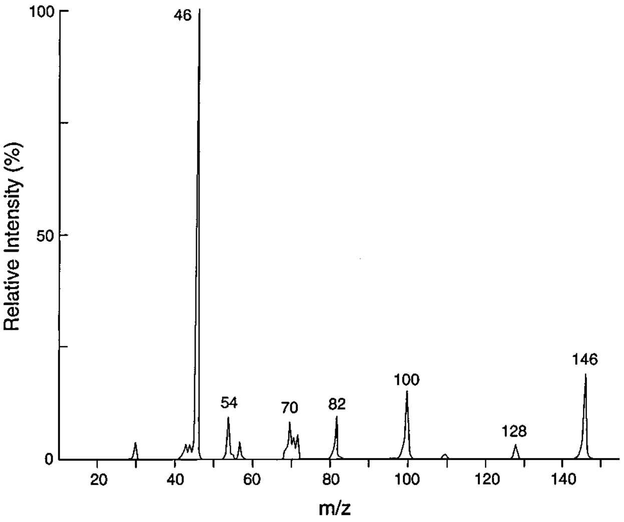

Figure 2. API-MS/MS daughter ion spectrum of the 146 u ion peak attributed to the $[M + H]^+$ ion of cyclohexyl nitrate.

1. Evidence for the formation of five of these seven potential products in the form of API-MS data of molecular ions, dominant fragment ions, and the presence of dimers, including heterodimers formed in the API-MS under the experimental conditions employed, is summarized in Table 1 together with additional confirmatory data (including MS/MS data). No evidence was found for the formation of 4-hydroxycyclohexanone (Scheme 3) or for the organic nitrate $HC(O)CH_2CH(ONO_2)CH_2CH_2CH_2OH$, which could be formed from reaction of the $HC(O)CH_2CH(OO^\bullet)CH_2CH_2CH_2OH$ radical with NO (Scheme 2).

Cyclohexyl nitrate and cyclohexyl nitrate-d_{11} were observed and quantified by GC-FID, as discussed below. Only relatively weak $[M + H]^+$ ions at masses 146 and 157 u for cyclohexyl nitrate and cyclohexyl nitrate-d_{11}, respectively, were observed in the API-MS spectra of the reaction products (Figure 1). An additional even-mass $[M + H]^+$ molecular ion at 162 u was attributed to $HC(O)CH_2CH_2CH_2CH_2CH_2ONO_2$. Although the molecular ions of these nitrates were weak, their identities were confirmed through API-MS/MS daughter ion spectra, which showed losses of 46 mass units (NO_2) and the presence of a strong 46 u fragment ion ($[NO_2]^+$) [see, for example, Figure 2 for the API-MS/MS daughter ion spectrum of cyclohexyl nitrate]. A heterodimer of $HC(O)CH_2CH_2CH_2CH_2CH_2ONO_2$ with the hydroxycarbonyl product, $HC(O)CH_2CH(OH)CH_2CH_2CHO$, was more readily observed in the API-MS spectrum shown in Figure 1A, and an API-MS/MS daughter ion spectrum of this dimer ion peak was consistent with the product assignments. As noted in Table 1, the corresponding deuterated nitrate was also observed, and the 312 u ion peak in Figure 1B is the heterodimer of $DC(O)CD_2CD_2CD_2CD_2CD_2ONO_2$ and $DC(O)CD_2CD(OH)CD_2CD_2CDO$ (Table 1).

Cyclohexanone and cyclohexanone-d_{12} were quantified by GC-FID, and API-MS/MS daughter and parent ion spectra confirmed their protonated molecular ions at 99 and 109 u, respectively, as well as the presence of numerous heterodimers (see Table 1). The hydroxydicarbonyl $HC(O)CH_2CH(OH)CH_2CH_2CHO$ (Scheme 2) showed a weak molecular ion $[M + H]^+$ at 131 u and a strong $[M + H - H_2O]^+$ fragment ion at 113 u in the API-MS spectrum and also showed heterodimer formation (Table 1). API-MS/MS daughter ion spectra of the 131 u ion peak (Figure 3A) showed a strong fragment ion at 113 u $[M + H - H_2O]^+$, consistent with the strong 113 u ion peak observed in the API-MS spectrum. The corresponding deuterated product from the cyclohexane-d_{12} reaction has an $[M + H]^+$ ion at 140 u due to rapid −OD to −OH exchange (Figure 3B). API-MS/MS daughter ion spectra of the 140 u ion peak (Figure 3B) showed a strong fragment ion at 122 u ($-H_2O$) and a weaker fragment at 121 u (−HDO), consistent with the strong 122 u ion peak observed in the API-MS analyses (loss of mainly H_2O and not HDO or D_2O is expected because of the presence of an −OH group).

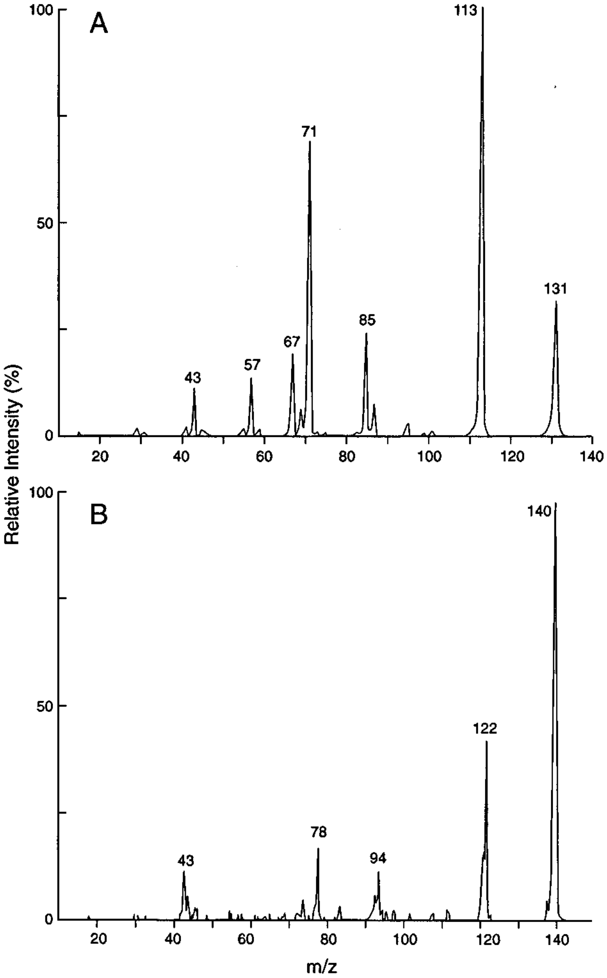

Figure 3. API-MS/MS daughter ion spectra of the 131 u (A) and 140 u (B) ion peaks attributed to the $[M + H]^+$ ions of $HC(O)CH_2CH(OH)CH_2CH_2CHO$ and $DC(O)CD_2CD(OH)CD_2CD_2CDO$ (after −OD to −OH exchange), respectively.

The two potential products $HC(O)CH_2CH_2CH_2CH_2CHO$ and 4-hydroxycyclohexanone both have molecular weights of 114 but may be distinguished through the cyclohexane-d_{12} reaction owing to the expected rapid −OD to −OH exchange for hydroxylated products, as previously observed.[20,21] There is evidence for the formation of the dialdehyde product, $HC(O)CH_2CH_2CH_2CH_2CHO$, but not for formation of 4-hydroxycyclohexanone. The API-MS/MS daughter ion spectra of the very weak 115 u protonated molecular ion peak (Figure 4A) showed fragment ions at 97 ($-H_2O$), 79 ($-2H_2O$), and 69 u ($-H_2O - CO$). The corresponding deuterated product ion occurred at 125 u, ruling out the formation of 4-hydroxycyclohexanone, which would have an $[M + H]^+$ ion at 124 u (due to rapid −OD to −OH exchange). Dimer ions provide confirming evidence (see Table 1) for this assignment.

GC-FID Analyses. As in previous studies of the reaction of the OH radical with cyclohexane in the presence of NO,[11,15,16] cyclohexanone and cyclohexyl nitrate (and their deuterated analogues from the cyclohexane-d_{12} reaction) were observed by GC-FID analyses and were confirmed by GC-MS analysis. The measured concentrations of cyclohexanone and cyclohexyl

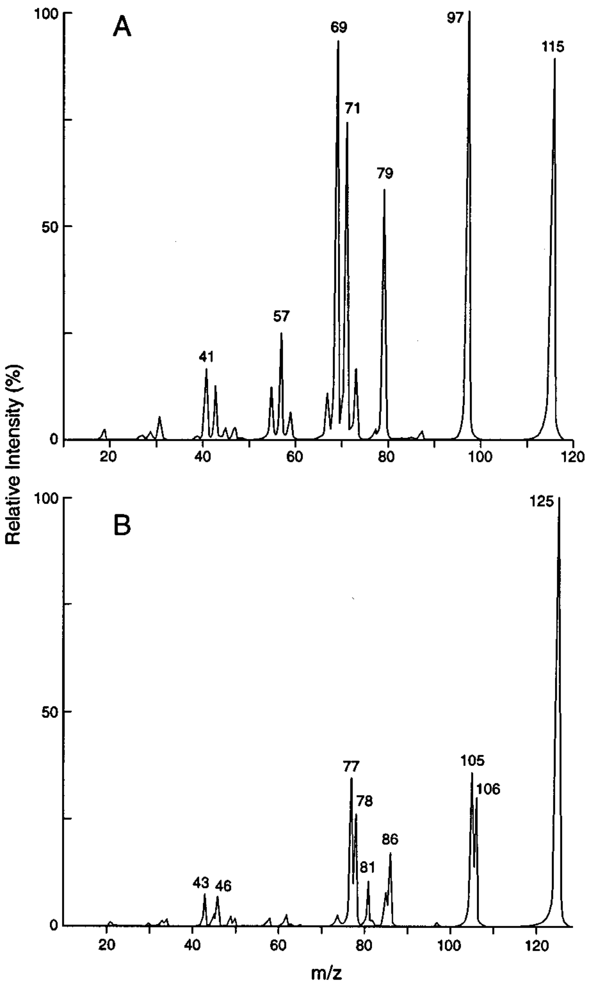

Figure 4. API-MS/MS daughter ion spectra of the 115 u (A) and 125 u (B) ion peaks attributed to the $[M + H]^+$ ions of $HC(O)CH_2CH_2CH_2CH_2CHO$ and $DC(O)CD_2CD_2CD_2CD_2CDO$, respectively.

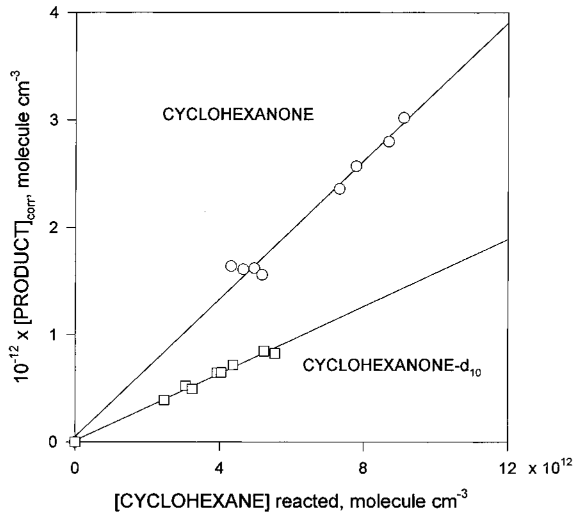

Figure 5. Plots of the amounts of cyclohexanone and cyclohexanone-d_{10} formed, corrected for reaction with the OH radical (see text), against the amounts of cyclohexane and cyclohexane-d_{12} reacted.

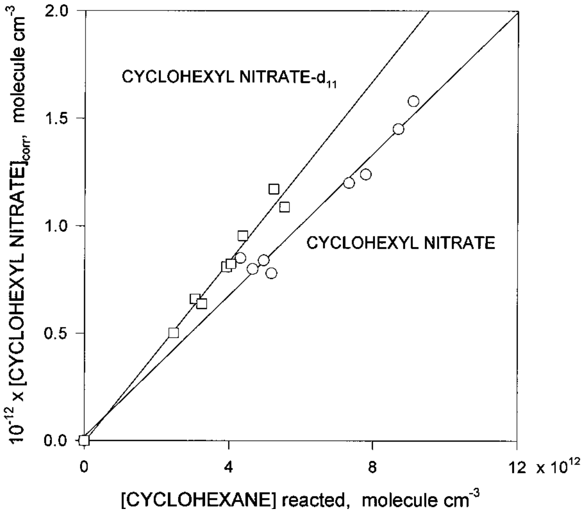

Figure 6. Plots of the amounts of cyclohexyl nitrate and cyclohexyl nitrate-d_{11} formed, corrected for reaction with the OH radical (see text), against the amounts of cyclohexane and cyclohexane-d_{12} reacted.

nitrate from the cyclohexane reaction were corrected to take into account secondary reactions with the OH radical.[25] By use of rate constants for the reactions of the OH radical with cyclohexane, cyclohexanone, and cyclohexyl nitrate (in units of 10^{-12} cm^3 molecule^{-1} s^{-1}) of 7.49,[9] 6.39,[26] and 3.30,[9,16] the multiplicative correction factors for secondary reactions with the OH radical, which increase with the rate constant ratio k(OH + product)/k(OH + cyclohexane) and with the extent of reaction, were $\leq$1.26 for cyclohexanone and $\leq$1.13 for cyclohexyl nitrate. Because no rate constants have been measured for the reactions of the OH radical with cyclohexanone-d_{10} or cyclohexyl nitrate-d_{11}, the rate constant ratios k(OH + cyclohexanone-d_{10})/k(OH + cyclohexane-d_{12}) and k(OH + cyclohexyl nitrate-d_{11})/k(OH + cyclohexane-d_{12}) were assumed to be identical with those for the nondeuterated species. The lower reactivity of cyclohexane-d_{12} compared to cyclohexane (by a factor of ~2.5 at 298 K[27]) led to a lower fraction of cyclohexane-d_{12} reacting ($\leq$23% for cyclohexane-d_{12} compared to $\leq$40% for cyclohexane), and the correction factors for secondary reaction in the cyclohexane-d_{12} system were lower than in the cyclohexane system, being $\leq$1.12 for cyclohexanone-d_{10} and $\leq$1.06 for cyclohexyl nitrate-d_{11}. Hence, the assumption of identical k(OH + product)/k(OH + reactant) ratios for the cyclohexane-d_{12} and cyclohexane reaction systems is expected to result in only small additional uncertainties (<10%).

Plots of the amounts of these products, corrected for reaction with the OH radical, against the amounts of cyclohexane and cyclohexane-d_{12} reacted are shown in Figures 5 (cyclohexanone and cyclohexanone-d_{10}) and 6 (cyclohexyl nitrate and cyclohexyl nitrate-d_{11}), respectively. The formation yields obtained from these data by least-squares analyses are given in Table 2. Our present formation yield for cyclohexanone from the cyclohexane reaction (0.321 ± 0.035) agrees within 10% with our previous measurement of 0.354 ± 0.042[15] and is in agreement within the uncertainties with the yield reported by Takagi et al.[11] (Table 2). Our present formation yield of cyclohexyl nitrate, arising from the reaction of the cyclohexyl peroxy radical with NO, of 0.165 ± 0.021 is in excellent agreement with our previous value of 0.160 ± 0.015[16] and is consistent within the large cited uncertainties[11] with the yield reported by Takagi et al.[11] (Table 2).

Our API-MS and API-MS/MS analyses show that isomerization of the cyclohexoxy radical (reaction Scheme 3) must be of minor or negligible importance, as may be expected because of the preferred chair conformation of the cyclohexoxy radical. Rather, the cyclohexoxy radical undergoes reaction with O_2, leading to cyclohexanone, and decomposition (reaction Schemes 1 and 2), with calculated reaction rates of 2.2×10^4 s^{-1} for the O_2 reaction at 298 K and 740 Torr total pressure of air and 6.3×10^4 s^{-1} for decomposition at 298 K[10] (Table 3). The $HC(O)CH_2CH_2CH_2CH_2CH_2O^\bullet$ alkoxy radical formed after the cyclohexoxy radical decomposition can decompose, isomer-

TABLE 2: Products Formed, and Their Formation Yields, from the Gas-Phase Reactions of the OH Radical with Cyclohexane and Cyclohexane-d_{12} in the Presence of NO at 298 ± 2 K and 740 Torr Total Pressure of Air

		formation yield	
reactant	product	this work[a]	lit
cyclohexane	cyclohexanone	0.321 ± 0.035	0.23 ± 0.13[b] 0.354 ± 0.042[a,c]
	cyclohexyl nitrate	0.165 ± 0.021	0.090 ± 0.044[b] 0.160 ± 0.015[d]
cyclohexane-d_{12}	cyclohexanone-d_{10}	0.156 ± 0.017	
	cyclohexyl nitrate-d_{11}	0.210 ± 0.025	

[a] Indicated errors are two least-squares standard deviations combined with estimated overall uncertainties in the GC-FID response factors for cyclohexane, cyclohexanone, and cyclohexyl nitrate of ±5% each. [b] Reference 11. Indicated error is one standard deviation. [c] Reference 15. [d] Reference 16. Indicated error is two least-squares standard deviations.

TABLE 3: Calculated Rates for the Decomposition and Reaction with O_2 of Cycloalkoxy Radicals at 298 K and 760 Torr Total Pressure of O_2 and Comparison of the Calculated and Experimentally Measured Cycloketone Formation Yields from Cycloalkoxy Radicals

	reaction rate (s^{-1})[a]		cycloketone yield	
cycloalkoxy radical	reaction with O_2	decompn	calcd	exptl
cyclopentoxy	5.6×10^4	2.9×10^6	0.019	0.017 ± 0.017[b]
cyclohexoxy	2.2×10^4	6.3×10^4	0.26	0.25 ± 0.15[b] 0.42 ± 0.06[c] 0.38 ± 0.05[d]
cycloheptoxy	1.3×10^5	1.4×10^6	0.085	0.033 ± 0.009[b]

[a] Calculated as discussed by Atkinson.[10] [b] Reference 11. Indicated error is one standard deviation. [c] References 15 and 16. [d] This work.

ize, or react with O_2.[9,10] Our API-MS and API-MS/MS data show that the $HC(O)CH_2CH_2CH_2CH_2CH_2O^{\bullet}$ radical preferentially isomerizes to yield the hydroxydicarbonyl $HC(O)CH_2CH(OH)CH_2CH_2CHO$, with the reaction with O_2 leading to $CHO(CH_2)_4CHO$ being of minor importance. These observations are consistent with estimated[10] rates of decomposition, isomerization, and reaction with O_2 of the $HC(O)CH_2CH_2CH_2CH_2CH_2O^{\bullet}$ radical at 298 K and 740 Torr total pressure of air, of 3.5×10^3, 2.6×10^6, and 3.1×10^4 s^{-1}, respectively, with the necessary thermochemical data being obtained from the NIST program[28] and Kerr.[29]

The deuterium isotope effect on the cyclohexanone formation yield (Table 2) is consistent with the intermediate cyclohexoxy radical reacting with O_2 in competition with decomposition via C−C bond scission, with the O_2 reaction involving H- (or D-) atom abstraction with a deuterium isotope effect and the decomposition pathway having no significant isotope effect. However, there is no marked deuterium isotope effect on the cyclohexyl nitrate formation yield, with the cyclohexyl nitrate-d_{11} yield from cyclohexane-d_{12} being a factor of 1.27 ± 0.23 higher than the cyclohexyl nitrate yield from cyclohexane, where the indicated error is two least-squares standard deviations. This observation is consistent with the reaction pathway forming cyclohexyl nitrate involving addition of NO to the cyclohexyl peroxy radical (reaction 3a) and with the reaction channels 3a and 3b both proceeding via an intermediate $[C_6H_{11}OONO]^*$ complex.[9] The only literature data to compare with our cyclohexyl nitrate yield data concern the rate constants for the reactions of $CH_3O_2^{\bullet}$ and $CD_3O_2^{\bullet}$ radicals with NO,[30,31] with measured rate constant ratios at room temperature of $k(CD_3O_2^{\bullet} + NO)/k(CH_3O_2^{\bullet} + NO) = 0.97 \pm 0.17$[30] and 1.15 ± 0.21,[31] consistent with our nitrate yield data.

The calculated[10] rates of decomposition and reaction with O_2 of the cyclopentoxy, cyclohexoxy, and cycloheptoxy radicals are given in Table 3, together with a comparison of the estimated and measured formation yields of cyclopentanone, cyclohexanone, and cycloheptanone from the corresponding cycloalkoxy radical. The ring-strain energies in the cyclopentoxy and cycloheptoxy radicals lead to significantly lower heats of reaction for decomposition than for the cyclohexoxy radical (with calculated values of ΔH_{decomp} of −1.1, 6.3, and 1.2 kcal mol^{-1} for the cyclopentoxy, cyclohexoxy, and cycloheptoxy radicals, respectively[28,29]), resulting in more rapid decomposition of the cyclopentoxy and cycloheptoxy radicals than for the cyclohexoxy radical (Table 3). The calculated rate of reaction of the cyclohexoxy radical with O_2 is lower than the rates of reaction with O_2 of the cyclopentoxy and cycloheptoxy radicals (Table 3). The calculated ratios of the rates of reaction with O_2 versus decomposition for the cyclopentoxy, cyclohexoxy, and cycloheptoxy radicals are in agreement with the experimental data (Table 3). Thus, reaction with O_2 and decomposition of the cyclohexoxy radical are competitive, while decomposition dominates for the cyclopentoxy and cycloheptoxy radicals (Table 3).

The products formed from the reaction of the OH radical with cyclohexane in the presence of NO are therefore cyclohexyl nitrate from the reaction of the cyclohexyl peroxy radical with NO, cyclohexanone from the cyclohexoxy radical reaction with O_2, and $HC(O)CH_2CH_2CH_2CH_2CH_2ONO_2$, $HC(O)CH_2CH_2CH_2CH_2CHO$, and $HC(O)CH_2CH(OH)CH_2CH_2CHO$ formed after the decomposition of the cyclohexoxy radical. Analogous products will be formed from cyclopentane and cycloheptane, except that the formation yields of cyclopentanone and cycloheptanone from cyclopentane and cycloheptane, respectively, are much lower than that of cyclohexanone from cyclohexane (Table 3). The products formed and the reaction schemes involved (Schemes 1 and 2 and analogous schemes for cyclopentane and cycloheptane), including the number of NO to NO_2 conversions involved in the product formation, can now be incorporated into chemical mechanisms for the atmospheric photooxidation of cycloalkanes and for more accurate calculation of their ozone-forming potentials. It is also possible that the multifunctional products $HC(O)CH_2CH_2CH_2CH_2CH_2ONO_2$, $HC(O)CH_2CH_2CH_2CH_2CHO$, and $HC(O)CH_2CH(OH)CH_2CH_2CHO$, and their homologues from the cyclopentane, cycloheptane, and other cycloalkane reactions, undergo gas/particle partitioning leading to secondary organic aerosol formation and/or are wet- and dry-deposited.

Acknowledgment. The authors gratefully thank the U.S. Environmental Protection Agency for supporting this research through Cooperative Agreement CR-821787-01-0 (Dr. Deborah J. Luecken, Project Officer) and Assistance Agreement R-825252-01-0 (Office of Research and Development) and thank the National Science Foundation (Grant No. ATM-9015361) and the University of California, Riverside, for funds for the purchase of the SCIEX API III MS/MS instrument. Although this research has been supported by the U.S. Environmental

Protection Agency, it has not been subjected to Agency review and, therefore, does not necessarily reflect the views of the Agency, and no official endorsement should be inferred.

References and Notes

(1) Lonneman, W. A.; Seila, R. L.; Meeks, S. A. *Environ. Sci. Technol.* **1986**, *20*, 790.

(2) Zweidinger, R. B.; Sigsby, J. E., Jr.; Tejada, S. B.; Stump, F. D.; Dropkin, D. L.; Ray, W. D.; Duncan, J. W. *Environ. Sci. Technol.* **1988**, *22*, 956.

(3) Lurmann, F. W.; Main, H. H. Analysis of the Ambient VOC Data Collected in the Southern California Air Quality Study; Sonoma Technology, Inc.: Santa Rosa, CA, 1992. Final Report to California Air Resources Board Contract No. A832-130, Sacramento, CA, February 1992; Sonoma Technology Inc.: Santa Rosa, CA, 1992.

(4) Hoekman, S. K. *Environ. Sci. Technol.* **1992**, *26*, 1206.

(5) Olson, K. L.; Sinkevitch, R. M.; Sloane, T. M. *J. Chromatogr. Sci.* **1992**, *30*, 500.

(6) Harley, R. A.; Cass, G. R. *Atmos. Environ.* **1995**, *29*, 905.

(7) Atkinson, R. *J. Phys. Chem. Ref. Data, Monogr. 1* **1989**, 1.

(8) National Research Council. *Rethinking the Ozone Problem in Urban and Regional Air Pollution*; National Academy Press: Washington, DC, 1991.

(9) Atkinson, R. *J. Phys. Chem. Ref. Data, Monogr. 2* **1994**, 1.

(10) Atkinson, R. *Int. J. Chem. Kinet.* **1997**, *29*, 99.

(11) Takagi, H.; Washida, N.; Bandow, H.; Okuda, M. *J. Phys. Chem.* **1981**, *85*, 2701.

(12) McEwen, C. N.; Druliner, J. D. *J. Am. Chem. Soc.* **1988**, *110*, 8579.

(13) Rowley, D. M.; Lightfoot, P. D.; Lesclaux, R.; Wallington, T. J. *J. Chem. Soc., Faraday Trans.* **1991**, *87*, 3221.

(14) Rowley, D. M.; Lightfoot, P. D.; Lesclaux, R.; Wallington, T. J. *J. Chem. Soc., Faraday Trans.* **1992**, *88*, 1369.

(15) Atkinson, R.; Aschmann, S. M.; Arey, J.; Shorees, B. *J. Geophys. Res.* **1992**, *97*, 6065.

(16) Atkinson, R.; Aschmann, S. M.; Carter, W. P. L.; Winer, A. M.; Pitts, J. N., Jr. *Int. J. Chem. Kinet.* **1984**, *16*, 1085.

(17) Atkinson, R.; Carter, W. P. L.; Winer, A. M.; Pitts, J. N., Jr. *J. Air Pollut. Control Assoc.* **1981**, *31*, 1090.

(18) Atkinson, R.; Aschmann, S. M. *Environ. Sci. Technol.* **1995**, *29*, 528.

(19) Atkinson, R.; Tuazon, E. C.; Aschmann, S. M. *Environ. Sci. Technol.* **1995**, *29*, 1674.

(20) Atkinson, R.; Kwok, E. S. C.; Arey, J.; Aschmann, S. M. *Faraday Discuss.* **1995**, *100*, 23.

(21) Kwok, E. S. C.; Arey, J.; Atkinson, R. *J. Phys. Chem.* **1996**, *100*, 214.

(22) Kwok, E. S. C.; Atkinson, R.; Arey, J. *Environ. Sci. Technol.* **1996**, *30*, 1048.

(23) Lau, Y. K.; Ikuta, S.; Kebarle, P. *J. Am. Chem. Soc.* **1982**, *104*, 1462.

(24) Kwok, E. S. C.; Arey, J. Manuscript in preparation.

(25) Atkinson, R.; Aschmann, S. M.; Carter, W. P. L.; Winer, A. M.; Pitts, J. N., Jr. *J. Phys. Chem.* **1982**, *86*, 4563.

(26) Dagaut, P.; Wallington, T. J.; Liu, R.; Kurylo, M. J. *J. Phys. Chem.* **1988**, *92*, 4375.

(27) Droege, A. T.; Tully, F. P. *J. Phys. Chem.* **1987**, *91*, 1222.

(28) Stein, S. E. *Structures and Properties Database and Estimation Program*, Version 2.0; National Institute of Standards and Technology Standard Reference Database 25; Chemical Kinetics and Thermodynamics Division, NIST: Gaithersburg, MD, 1994.

(29) Kerr, J. A. Strengths of Chemical Bonds. In *Handbook of Chemistry and Physics*, 74th ed.; Lide, D. R., Ed.; CRC Press: Boca Raton, FL, 1993−94.

(30) Masaki, A.; Tsunashima, S.; Washida, N. *Chem. Phys. Lett.* **1994**, *218*, 523.

(31) Helleis, F.; Moortgat, G. K.; Crowley, J. N. *J. Phys. Chem.* **1996**, *100*, 17846.